

Theory of transient spontaneous emission by an atom in a planar microcavity

Ottavia Jedrkiewicz and Rodney Loudon

Physics Department, Essex University, Colchester CO4 3SQ, United Kingdom

(Received 19 April 1999)

We study the transient regime of spontaneous emission by an atom excited in a planar high- Q microcavity. The variation of the spatial distribution of the radiation outside the cavity is determined as a function of the increasing number of internal reflections for transition dipole moments parallel and perpendicular to the mirrors and for mirror separations equal to $\lambda/2$ and $\lambda/4$. Particular attention is given to the parallel dipole in the $\lambda/2$ cavity, where the number of reflections is closely proportional to the elapsed time. It is shown that the transient regime extends over times of the order of the cavity decay time, in contrast to the effectively one-dimensional cavities previously studied, where the steady state is achieved after the cavity round-trip time. The field distribution inside the cavity tends to a steady-state form whose dimension parallel to the mirrors is of the order of the transverse coherence length. Despite this transverse localization of the field excitation, it is shown that the conditions for the achievement of strong atom-field coupling and the observation of Rabi oscillations cannot be met in the planar microcavity. [S1050-2947(99)06911-5]

PACS number(s): 42.50.Ct, 42.50.Md, 32.80.-t

I. INTRODUCTION

Calculations of the radiation of light by atoms placed in microcavities normally begin with analyses of the field modes appropriate to the cavity geometry. These modes have well-defined spatial structures, determined essentially by classical electromagnetic theory, with standard boundary conditions at the surfaces of the cavity mirrors. They form a convenient basis for calculations of the dynamics of the coupled system of atomic transition and radiation field, especially the exchanges of energy between atoms prepared in given initial states and the field. The state of the coupled system in these processes is, of course, time dependent, but the coupling Hamiltonian itself is independent of the time.

Extensions to this approach to calculations in cavity quantum electrodynamics are needed in the very initial stages of radiative processes, particularly spontaneous emission. We consider an excited atom that is injected into the center of a symmetrical cavity at time $t=0$. It follows from general principles of relativistic causality that the atom is not immediately aware of its surroundings. Thus the atom begins to radiate as it would in free space, and it is only after the time τ_{rt} needed for a round trip to the cavity mirrors and back with velocity c that the time development of the atomic excitation level is changed from its free-space form. Explicit calculations for spherical [1] and one-dimensional [2] cavities find an initial exponential decay at the free-space rate. The behavior begins to convert to a more complicated time dependence at time τ_{rt} , and, for appropriate values of the atomic and cavity parameters, the characteristic vacuum Rabi oscillations are established at longer times.

The purpose of the present paper is to extend the work on initial transient emission by atoms in spherical and one-dimensional cavities to planar microcavities, which consist of a pair of plane-parallel mirrors in a three-dimensional space. Although several cases are illustrated, the main calculations refer to an atomic dipole oriented parallel to the mirrors with cavity length d related to the emission wavelength λ by $d=\lambda/2$. We show that the time development in the

planar geometry is quite different from that in other shapes of cavity, for example spherical, one dimensional, and confocal. Thus the transient regime generally persists over a longer time scale, controlled by the cavity decay time τ_c rather than the round-trip time τ_{rt} . The cavity excitation established by the end of the regime also occupies a much larger volume, determined by the transverse coherence length of the planar microcavity, a concept introduced by De Martini *et al.* [3] and developed by Ujihara [4]. The transient behavior is difficult to detect in experiments, because of its relative brevity, but its form confirms important matters of principle in the causal time development of quantum-mechanical systems.

A study of the transient behavior is also important in understanding the conditions for the subsequent occurrence, or not, of vacuum Rabi oscillations. The conditions of experiments with high- Q microcavities ensure that the round-trip time τ_{rt} is much shorter than the cavity decay time τ_c ; it is also usually much shorter than the free-space atomic radiative lifetime τ_{rad} . Vacuum Rabi oscillations of frequency Ω may occur when the transition is coupled to a single longitudinal mode of the cavity, with a coupling constant denoted $\Omega/2$. It is necessary for the occurrence of oscillations that the Rabi period is much shorter than the cavity decay time and the residual radiative lifetime in the cavity; this is referred to as the strong-coupling regime. The weak-coupling regime is defined by the opposite conditions of a long Rabi period, when the vacuum oscillations are quenched. We shall show that these conditions also determine the forms of initial transient behavior, and that vacuum Rabi oscillations are difficult to achieve in the planar geometry.

The calculations begin in Sec. II with a brief review of the main results for the steady-state modes in a high- Q planar cavity and their adaptation to the study of transient effects in the weak-coupling regime. We derive the dependences of the intensity patterns radiated outside the cavity on the numbers of internal reflections for initially excited atoms with parallel and perpendicular dipole orientations, and for two characteristic microcavity lengths. The external radiation patterns are

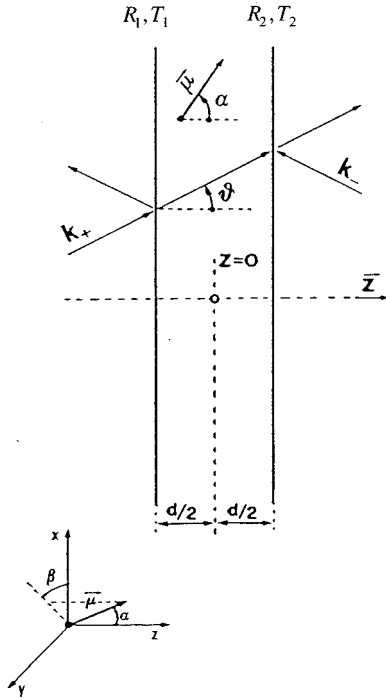


FIG. 1. Geometry of the Fabry-Perot microcavity showing the notations for coordinate axes, mirror coefficients, mode wave vectors, and dipole orientation.

analyzed in Sec. III in terms of their angular divergence. The transient behavior of the field excitation inside the cavity is determined, and it is shown to lead to the steady-state coherence length and mode volume found previously [3,4]. The main calculations assume a symmetrical microcavity, but in Sec. IV we make comparisons with previous work on emission by atoms close to a single plane mirror [5,6]. The conditions for the achievement of the strong-coupling regime and the observation of vacuum Rabi oscillations are discussed in Sec. V; the unfavorable possibilities of the planar cavity are contrasted with those of the confocal cavity, and compared with the situations in other forms of symmetrical cavity. The main conclusions are summarized in Sec. VI.

II. TIME DEPENDENCE OF THE RADIATED INTENSITY

The quantum theory of spontaneous emission by an atom in a microscopic planar cavity was derived in previous work [7] by considering a complete set of orthonormal mode functions that span the infinite three-dimensional vacuum that pervades and surrounds the microcavity. The geometry of the cavity is shown in Fig. 1. The electromagnetic field is quantized by the introduction of creation and destruction operators associated with the mode functions. The wave vectors \vec{k}_+ and \vec{k}_- associated with plane waves of unit amplitude incoming from the left and right sides of the cavity are functions of the polar angles θ and ϕ :

$$\begin{aligned}\vec{k}_+ &= k(\sin \theta \cos \phi, \sin \theta \sin \phi, \cos \theta), \\ \vec{k}_- &= k(\sin \theta \cos \phi, \sin \theta \sin \phi, -\cos \theta),\end{aligned}\quad (1)$$

where $0 \leq \theta \leq \pi/2$ and $0 \leq \phi < 2\pi$. Orthonormal polarization vectors are defined for each wave vector by

$$\vec{\epsilon}(\vec{k}_+, 1) = \vec{\epsilon}(\vec{k}_-, 1) = (\sin \phi, -\cos \phi, 0),$$

$$\vec{\epsilon}(\vec{k}_+, 2) = (\cos \theta \cos \phi, \cos \theta \sin \phi, -\sin \theta),$$

$$\vec{\epsilon}(\vec{k}_-, 2) = (\cos \theta \cos \phi, \cos \theta \sin \phi, \sin \theta), \quad (2)$$

where index 1 is associated with the *s*-wave component (polarized orthogonal to the incident plane) and index 2 with the *p*-wave component (polarized parallel to the incident plane). The polarization index is denoted in general by $j=1, 2$. The emitting dipole is localized for simplicity at $\vec{r}_0=0$ inside the cavity, with orientation

$$\vec{\mu} = \mu(\sin \alpha \cos \beta, \sin \alpha \sin \beta, \cos \alpha). \quad (3)$$

The cavity mirrors are assumed to be metallic with zero effective thicknesses and infinite extents in the *xy* plane. The complex reflection and transmission coefficients $R_{1,2}$ and $T_{1,2}$ of the first and second cavity mirrors are assumed independent of polarization, frequency, and incidence angle over the range considered, and with constant phase shifts [8]. They satisfy $|R_i|^2 + |T_i|^2 = 1$ and $R_i^* T_i + R_i T_i^* = 0$ ($i=1$ and 2).

The spatial mode functions of the field are associated with plane waves of unit amplitude incident externally from the left and right of the cavity. They are derived, as usual in Fabry-Perot theory, by summing the geometric series resulting from the multiple reflections on the mirrors [8]. In the *steady-state* regime and *inside* the planar cavity, the form of spatial dependence of the field incident from the left for polarization j is [7]

$$\begin{aligned}D^{-1}\{T_1 \exp(i\vec{k}_+ \cdot \vec{r}) \vec{\epsilon}(\vec{k}_+, j) \\ + T_1 R_2 \exp[i\vec{k}_- \cdot \vec{r} + ikd \cos \theta] \vec{\epsilon}(\vec{k}_-, j)\} - \frac{1}{2}d < z < \frac{1}{2}d,\end{aligned}\quad (4)$$

where d is the mirror separation. The form of spatial dependence of the field incident from the right is given by a similar expression but with interchanges of subscripts 1 with 2 and + with -. The Airy function is defined by

$$\begin{aligned}D^{-1} &= \sum_{n=0}^{\infty} (R_1 R_2)^n \exp(2iknd \cos \theta) \\ &= 1/\{1 - R_1 R_2 \exp(2ikd \cos \theta)\}.\end{aligned}\quad (5)$$

The total field amplitude at the location of the atom inside the cavity at $\vec{r}_0=0$, derived by summing the contributions of all the modes, is used to obtain the spontaneous emission rate of the atom by Fermi's golden rule.

The spatial dependence of the intensity per unit solid angle radiated by the dipole is derived, as in a classical description, by addition of all the partial emitted plane waves to form the total interference pattern. The radiated field *outside* the cavity on the right has a spatial dependence,

$$\begin{aligned}D^{-1}\{T_2 \exp(i\vec{k}_+ \cdot \vec{r}) \vec{\epsilon}(\vec{k}_+, j) + T_2 R_1 \\ \times \exp[i\vec{k}_- \cdot \vec{r} + ikd \cos \theta] \vec{\epsilon}(\vec{k}_-, j)\}, \\ \frac{1}{2}d < z,\end{aligned}\quad (6)$$

similar to Eq. (4) but with the mirror labels interchanged. The square modulus of this expression gives the radiated intensity per unit solid angle on the right of the cavity for a given polarization, proportional to the corresponding spontaneous emission rate per unit solid angle. The spatial dependence of the radiated field on the left of the cavity is given by Eq. (6) with interchanges of subscripts 1 and 2 and + with -.

In order to study the *transient* regime of the atomic dynamics and its effect on the establishment of the radiation pattern, we need the time dependence of the field self-interference process. This is related to the geometrical sum in Eq. (5) restricted to a finite number N of reflections, with the Airy function replaced by

$$\sum_{n=0}^N (R_1 R_2)^n \exp(2iknd \cos \theta) = \frac{1 - (R_1 R_2)^{(N+1)} \exp(2ik(N+1)d \cos \theta)}{1 - R_1 R_2 \exp(2ikd \cos \theta)}. \quad (7)$$

We shall show that the description of the atomic dynamics in terms of the number N of reflections is closely equivalent to a description in the time domain for emission by a dipole oriented parallel to the mirrors and a mirror separation related to the emission wavelength by $d = \lambda/2$. In this case, one reflection occurs every roundtrip time τ_{rt} to a good approximation for the relatively small propagation angles θ of the radiation inside the cavity, and the time associated with one reflection is given by

$$\tau_{\text{ref}} = d/(c \cos \theta) \rightarrow \tau_{\text{rt}} = d/c \quad \text{for } \theta \rightarrow 0. \quad (8)$$

For an atom excited at time $t=0$, the establishment of the radiation pattern as a function of N is thus a good indicator of the buildup of the cavity-field mode in the transient regime of the spontaneous emission process. The relation between the N and t dependences is less direct for the other examples considered, where the radiation is not confined to small angles θ .

We consider a dipole parallel to the mirrors of a $d = \lambda/2$ microcavity in Sec. II A, and compare the results with those for a dipole orthogonal to the mirrors in Sec. II B. In Sec. II C, we analyze the emission by an atomic dipole parallel and orthogonal, respectively, to the mirrors of a $d = \lambda/4$ microcavity.

A. Dipole parallel to the mirrors of a resonant cavity

We assume a *symmetrical* resonant microcavity with mirrors whose reflection and transmission coefficients are equal, $R_{1,2} = R = -|R|$ and $T_{1,2} = T = i|T|$, respectively. The mirror separation is related to the emission wavelength by $d = \lambda/2$ and to the wave vector by $kd = \pi$. The atom is placed in the center of the cavity with its dipole parallel to the x axis. The radiated intensity per unit solid angle as a function of N , in units of $3/4\pi$, is determined by the square modulus of the emitted field amplitude after N reflections as

$$\begin{aligned} \frac{I_{\parallel}(\theta, \phi, N)}{I_0} &= \frac{1 + |R|^{4(N+1)} - 2|R|^{2(N+1)} \cos(2\pi(N+1) \cos \theta)}{1 + |R|^4 - 2|R|^2 \cos(2\pi \cos \theta)} \\ &\times |T|^2 \{1 + |R|^2 - 2|R| \cos(\pi \cos \theta)\} \\ &\times \{\sin^2 \phi + \cos^2 \phi \cos^2 \theta\}, \end{aligned} \quad (9)$$

where Eqs. (2), (6) and (7) have been used, and I_0 is the free-space spontaneous emission intensity integrated over the half-space solid angle. With this normalization, the free-space radiation pattern derived from Eq. (9) by setting $|R|^2 = 0$ has a unit value in the direction orthogonal to the mirrors with $\theta=0$. Note that the two terms in the final bracket give the contributions from the s and p -polarized fields, respectively. By setting $\phi=0$ or $\pi/2$, we obtain expressions describing the progressive establishment of the radiation pattern in the zx and yz planes, respectively. For $N=0$ the only contribution to the interference pattern comes from the superposition of the wave propagating toward one mirror and the counterpropagating wave reflected by the other mirror to give the intensity distribution established after one round-trip time.

Figure 2 illustrates the progressive modifications of the radiation patterns in the zx and yz planes, respectively, as functions of the number of multiple reflections. The radiation intensity per unit solid angle is plotted as a function of the propagation angle θ , for different values of N . Mirrors with very high reflectivity are assumed. The dipole initially emits as in free space for times shorter than the round-trip time, and it is at the time of arrival of the light reflected back from the mirror that the atom first acquires information about the boundary, as previously noticed [1,2]. However, it is also clear from these results that the round-trip time is not sufficient for the field mode to be completely established in a planar cavity. We can say that, after each reflection of the field at the cavity walls, the atom ‘‘feels’’ the boundaries a little bit more and progressively adapts its further deexcitation dynamics to the conditions imposed by the geometry of the system and the dipole orientation. Note how the small initial anisotropy of the spatial intensity distribution, due to the dependence on ϕ , vanishes very quickly for increasing values of N as $\cos \theta$ tends to 1. In the steady-state regime, characterized by a strong enhancement of the emission in the direction orthogonal to the mirrors, the propagation angle θ tends to zero, and the projection of the emission lobe on the xy plane (pattern seen from the z axis) has the shape of a very small diameter disk.

The steady-state radiation pattern is described by a normalized intensity distribution obtained from Eq. (9) for $N \rightarrow \infty$ as

$$\begin{aligned} \frac{I_{\parallel}(\theta, \phi)}{I_0} &= \frac{|T|^2 \{1 + |R|^2 - 2|R| \cos(\pi \cos \theta)\}}{1 + |R|^4 - 2|R|^2 \cos(2\pi \cos \theta)} \\ &\times \{\sin^2 \phi + \cos^2 \phi \cos^2 \theta\}. \end{aligned} \quad (10)$$

This is also proportional to the spontaneous emission rate per unit solid angle. In the weak-coupling regime, the total spontaneous emission rate for a dipole parallel to the x axis and

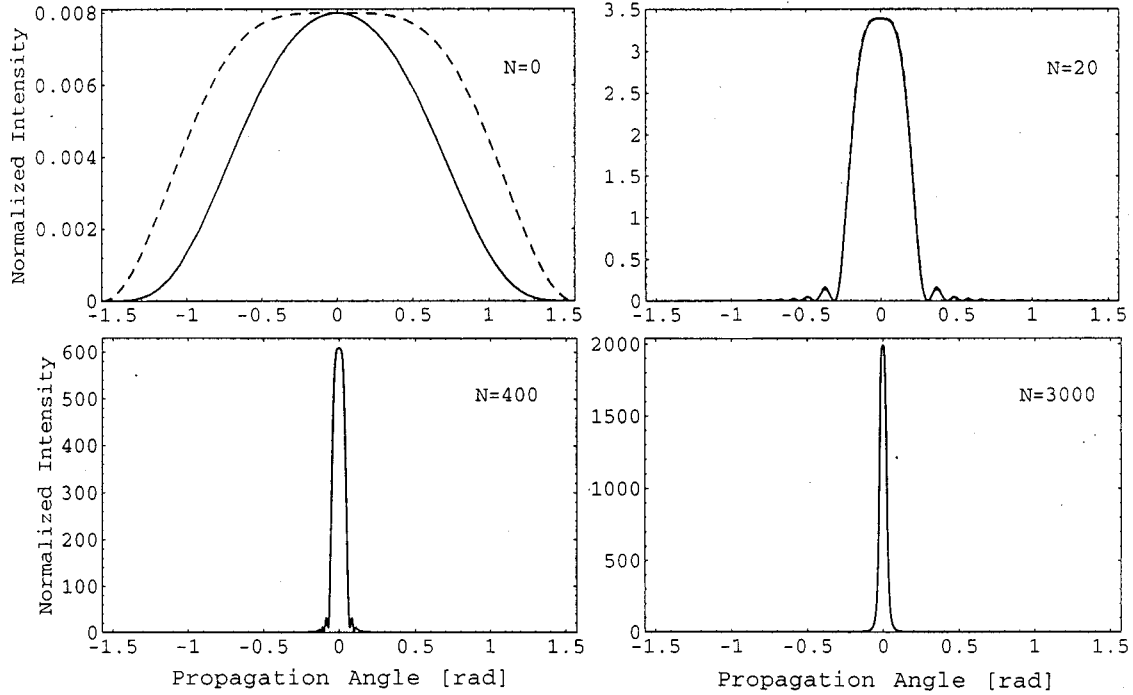


FIG. 2. External radiation pattern from a dipole parallel to the mirrors of a cavity with $d=\lambda/2$ and $|R|^2=0.998$, after the numbers N of reflections indicated. The continuous and broken curves refer to the xz and yz planes, respectively.

placed in the middle of the cavity, evaluated from Fermi's golden rule [7,9], can be written as

$$\Gamma_{\parallel} = \frac{3}{4\pi} \Gamma_0 \int_0^{\pi/2} \sin \theta d\theta \int_0^{2\pi} d\phi I_{\parallel}(\theta, \phi)/I_0, \quad (11)$$

where Γ_0 is the emission rate in free space. The relative spontaneous-emission rate is thus directly related to the ratio of radiated intensities given by Eq. (10), expressed in units of $3/4\pi$.

The intensity distribution given by Eq. (10) simplifies in the limit of a perfect cavity with zero-transmission mirrors. As $\theta \rightarrow 0$ when $|R|^2 \rightarrow 1$, we can expand the function $\cos \theta$ around 1, and obtain the radiation pattern in any plane orthogonal to the mirrors as

$$\frac{I_{\parallel}(\theta)}{I_0} = \frac{|T|^2(1+|R|^2)^2}{(1-|R|^2)^2 + \pi^2|R|^2\theta^4} \approx \frac{4|T|^2/\pi^2}{(|T|^2/\pi)^2 + \theta^4}. \quad (12)$$

This shows an enhancement of $4/|T|^2$ relative to the small-angle intensity in the absence of the mirrors ($|R|=0$). The evaluation of the angular divergence at half the maximum of the emitted intensity leads to the well-known result [3,10,11]

$$\Delta \theta \cong \frac{2}{[\pi/(1-|R|^2)]^{1/2}} = \frac{2|T|}{\sqrt{\pi}}. \quad (13)$$

The angular divergence tends to zero for $|T| \rightarrow 0$ and, in this limit, a well-known representation of Dirac's delta function leads to

$$I_{\parallel}(\theta)/I_0 \cong 4\delta(\theta^2). \quad (14)$$

The integrated spontaneous emission intensity thus remains constant on the approach to perfect reflectivity, as the increase in peak intensity is compensated by the decrease in the divergence angle of the emission lobe.

Using representation (14), the evaluation of the spontaneous emission rate for a dipole parallel to the x axis is now straightforward, and from Eq. (11) setting $\sin \theta \cong \theta$, we have

$$\Gamma_{\parallel} = \frac{3}{4\pi} \Gamma_0 \int_0^{2\pi} d\phi \int_0^{\pi/4} d\theta^2 \frac{1}{2} 4\delta(\theta^2) = \frac{3}{2} \Gamma_0. \quad (15)$$

The spontaneous emission lifetime is reduced by a factor of $\frac{2}{3}$, in agreement with previous work [10]. A direct integration of Eq. (14) over the half-space, with the real units of the normalized intensity distribution restored, shows that the energy per unit time radiated by the atom is increased by a factor of $\frac{3}{2}$, which compensates for the reduction of the atomic decay time and ensures the conservation of energy. It is worth noting that a more general evaluation of the spontaneous emission rate of a dipole parallel to the mirrors, as a function of kd , shows that a maximum value $\Gamma_{\parallel} = 3\Gamma_0$ is reached as soon as kd is slightly greater than π for $|R|^2 \rightarrow 1$ [7,12–17]. In fact, $kd = \pi$ is a cutoff value due to the boundary conditions of the electromagnetic field in a cavity with perfect reflecting mirrors, and formally $\Gamma_{\parallel} = 3\Gamma_0$ occurs only in the limit $d \rightarrow \lambda/2$.

B. Dipole orthogonal to the mirrors of a resonant cavity

We now consider an atomic dipole oriented parallel to the z axis in the middle of a $d=\lambda/2$ symmetrical microcavity. Only the p -polarized field contributes, and the normalized intensity distribution after N reflections is

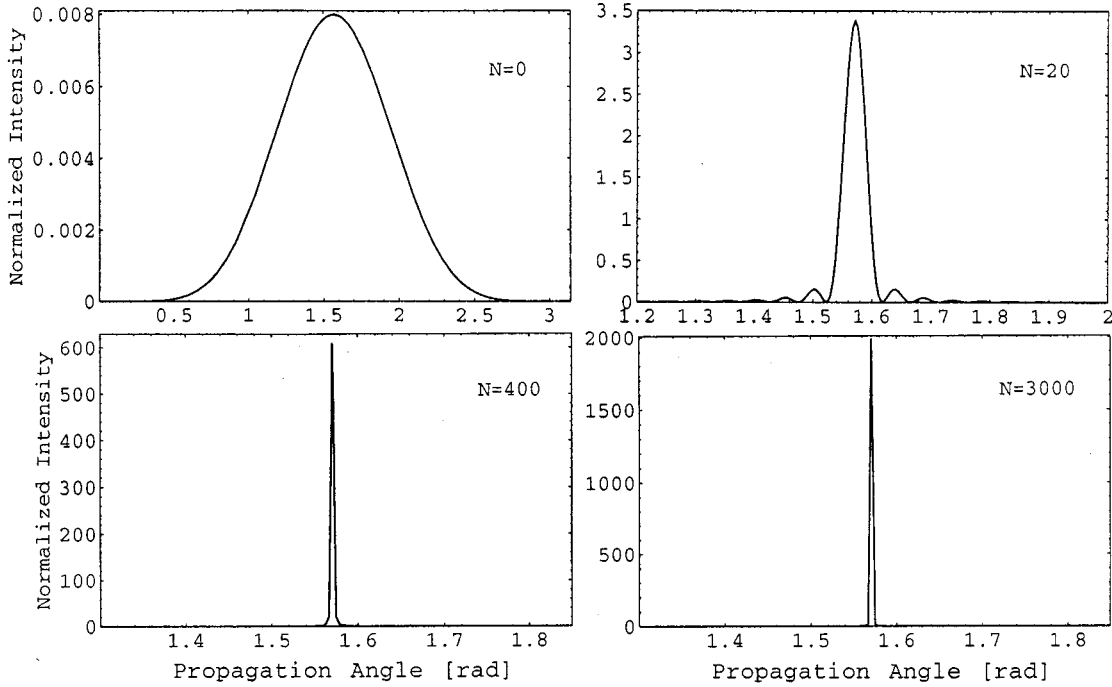


FIG. 3. External radiation patterns as in Fig. 2 but for a dipole perpendicular to the mirrors. The intensity is isotropic around the z axis.

$$\frac{I_{\perp}(\theta, N)}{I_0} = \frac{1 + |R|^{4(N+1)} - 2|R|^{2(N+1)} \cos(2\pi(N+1)\cos\theta)}{1 + |R|^4 - 2|R|^2 \cos(2\pi \cos\theta)} \times |T|^2 \{1 + |R|^2 + 2|R| \cos(\pi \cos\theta)\} \sin^2\theta. \quad (16)$$

The emission is independent of the angle ϕ , and absolutely isotropic in the xy plane. The emission intensity is now concentrated around $\theta = \pi/2$, and the dipole radiates in all directions parallel to the mirrors. Figure 3 shows the spatial pattern of the emission in any plane orthogonal to the mirrors and containing the z axis, for increasing values of N . The axis is centered on $\theta = \pi/2$ in order to show the entire intensity pattern, and the relation of N to the elapsed time is ill defined. However, the round-trip time is clearly not sufficient for the dipole to completely “feel” the boundaries, and the final field pattern cannot be established in this time.

The normalized intensity distribution in the steady-state regime is obtained from Eq. (16), with $N \rightarrow \infty$, as

$$\frac{I_{\perp}(\theta)}{I_0} = \frac{|T|^2 \{1 + |R|^2 + 2|R| \cos(\pi \cos\theta)\}}{1 + |R|^4 - 2|R|^2 \cos(2\pi \cos\theta)} \sin^2\theta. \quad (17)$$

The spontaneous emission rate of an atomic dipole orthogonal to the mirrors of a symmetrical cavity is again given by Eq. (11) but with $I_{\parallel}(\theta, \phi)$ replaced by $I_{\perp}(\theta)$. In the limit of perfect mirrors, where $|R|^2 \rightarrow 1$, Eq. (17) can be expanded around $\theta = \pi/2$. To a good approximation,

$$\begin{aligned} \frac{I_{\perp}(\theta)}{I_0} &= \frac{|T|^2(1 + |R|^2)^2}{(1 - |R|^2)^2 + 4\pi^2|R|^2 \left(\theta - \frac{1}{2}\pi\right)^2} \\ &\approx \frac{|T|^2/\pi^2}{(|T|^2/2\pi)^2 + \left(\theta - \frac{1}{2}\pi\right)^2}, \end{aligned} \quad (18)$$

again showing an enhancement of $4|T|^2$ relative to free-space emission at $\theta = \pi/2$. The angular divergence at half maximum intensity is

$$\Delta\theta \cong \frac{1 - |R|^2}{\pi} = \frac{|T|^2}{\pi}, \quad (19)$$

in agreement with previous results [10]. Comparison of Eqs. (19) and (13) shows that the planar lobe of the enhanced emission of a dipole orthogonal to the mirrors for small values of $|T|$ is much narrower than the unidirectional emission lobe of a dipole parallel to the mirrors.

For $|T|^2 \rightarrow 0$, (18) takes the limiting form

$$\frac{I_{\perp}(\theta)}{I_0} \cong 2\delta\left(\theta - \frac{\pi}{2}\right). \quad (20)$$

Using Eq. (20), we easily evaluate the spontaneous emission rate for a perpendicular dipole, replacing \parallel by \perp and putting $\sin\theta \cong 1$ in Eq. (11). We thus obtain, in agreement with previous results [7,10,15,16],

$$\Gamma_{\perp} = \frac{3}{4\pi} \Gamma_0 \int_0^{2\pi} d\phi \int_0^{\pi/2} d\theta \delta\left(\theta - \frac{\pi}{2}\right) = \frac{3}{2} \Gamma_0. \quad (21)$$

The spontaneous emission lifetime is reduced by a factor of $\frac{2}{3}$ with respect to the free-space value, as for the emission of the dipole parallel to the mirrors. The energy of the system is again conserved.

C. Spontaneous emission in a cavity where $d < \lambda/2$

We now consider a symmetrical planar microcavity with a smaller mirror separation, namely, $d = \lambda/4$ or $kd = \pi/2$, than that of the two preceding subsections. We analyze the establishment of the intensity distribution for a dipole parallel to

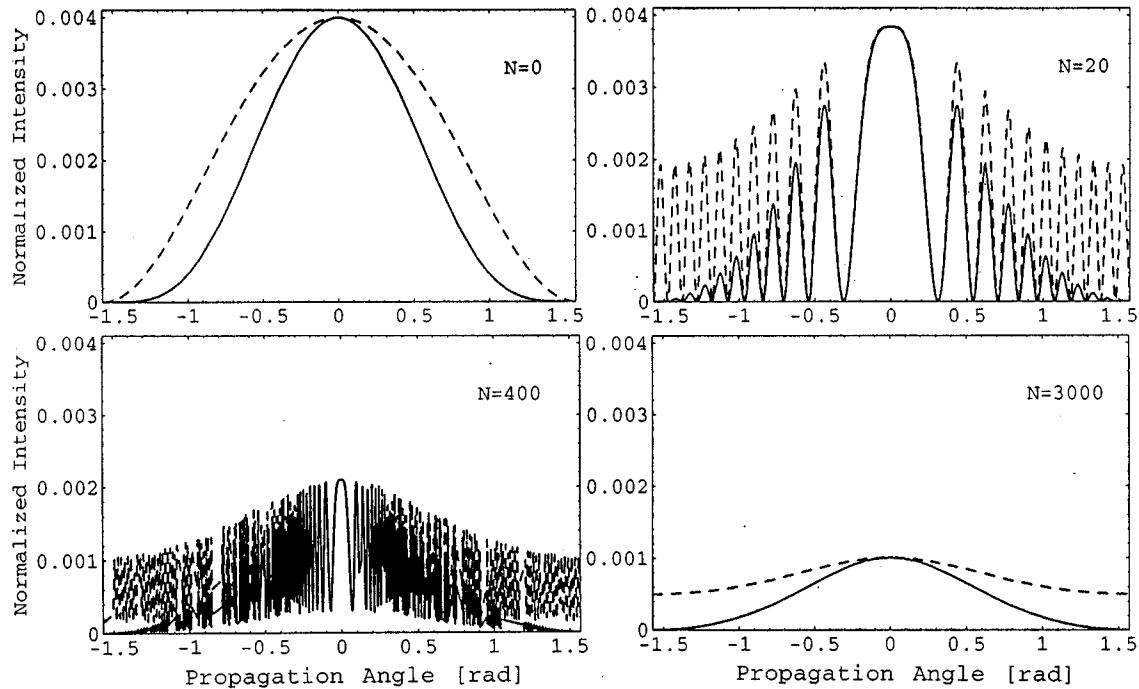


FIG. 4. External radiation patterns for a dipole parallel to the mirrors as in Fig. 2, but with mirror separation $d=\lambda/4$.

the mirrors and then for a dipole orthogonal to the mirrors, again assuming a weak-coupling regime.

For an atomic dipole parallel to the x axis, the normalized radiated intensity per unit solid angle, as a function of the number N of reflections, is given by Eq. (9) but with π everywhere replaced by $\pi/2$. The transient effect is illustrated in Fig. 4, where we plot the spatial intensity distributions in the zx and yx planes as functions of the propagation angle θ . The oscillating dipole radiates as in free space before the first round-trip of the electromagnetic wave. The further radiative evolution of the atom is progressively modified after subsequent field reflections, until inhibition of the emission occurs for $N \rightarrow \infty$, when the spontaneous emission rate is drastically reduced. The peak radiated intensity at $\theta = 0$ in the steady state for $d=\lambda/4$ is given in general by

$$\frac{I_{\parallel}(0)}{I_0} = \frac{1 - |R|^2}{1 + |R|^2}, \quad (22)$$

and complete inhibition occurs for perfectly reflecting mirrors [16].

In terms of the classical picture of dipole images [18,19], we note that for a dipole parallel to the perfectly reflecting mirrors and a mirror separation shorter than half the atomic wavelength, the sum of the radiation emitted by the images completely cancels the radiation emitted by the real dipole. Separations $d < \lambda/2$ thus correspond to conditions of destructive self-interference for the reflected waves of the emitted radiation. Alternatively, considering the excited atom as stimulated by the vacuum field, the only available modes for $d < \lambda/2$ do not interact with the dipole, as their polarization is orthogonal to the mirrors, and the emission is inhibited. When $|R|^2 \neq 1$, the emission in the steady state is not completely suppressed because of the existence of other modes whose polarization is not orthogonal to the atomic dipole.

The spontaneous emission rate for $d=\lambda/4$ is given by Eq. (11), with substitution of a modified form of Eq. (10) in which π is replaced by $\pi/2$. In the limit $|R|^2 \rightarrow 1$, the result is approximately

$$\begin{aligned} \Gamma_{\parallel} &\cong \frac{3}{4} \Gamma_0 |T|^2 \int_0^{\pi/2} d\theta \sin \theta \frac{1 - \cos((\pi/2) \cos \theta)}{1 - \cos(\pi \cos \theta)} \{1 + \cos^2 \theta\} \\ &\propto \Gamma_0 |T|^2, \end{aligned} \quad (23)$$

as the integral is convergent, and Γ_{\parallel} tends to zero for $|R|^2 \rightarrow 1$ or $|T|^2 \rightarrow 0$.

For $d \ll \lambda/2$ we put $kd \approx 0$ in Eqs. (6) and (7), and replace π by 0 in Eq. (10) to obtain the spontaneous emission rate (11) for a general value of $|R|$ as

$$\Gamma_{\parallel} \cong \Gamma_0 \frac{|T|^2 (1 - |R|^2)^2}{(1 - |R|^2)^2} = \Gamma_0 \frac{1 - |R|}{1 + |R|}. \quad (24)$$

When $|R|^2 \rightarrow 1$, $\Gamma_{\parallel} \cong \Gamma_0 |T|^2/4$, in agreement with previous results [7]. Although the condition $d \ll \lambda/2$ is difficult to realize in the optical regime, we can say in general that when the oscillating dipole is placed in a cavity shorter than half the emission wavelength and is oriented parallel to the mirrors, the spontaneous emission lifetime of the atom tends to infinity for reflectivities tending to unity. Spontaneous emission does take place for reflectivities not quite equal to unity, but it is a really very slow process.

For an atomic dipole perpendicular to the mirrors of a $d = \lambda/4$ microcavity, the normalized radiated intensity per unit solid angle, as a function of the number N of reflections, is given by Eq. (16), but with π everywhere replaced by $\pi/2$. The intensity distribution in any plane orthogonal to the mirrors, and containing the z axis, is illustrated in Fig. 5 for different values of N . There is now a constructive interfer-

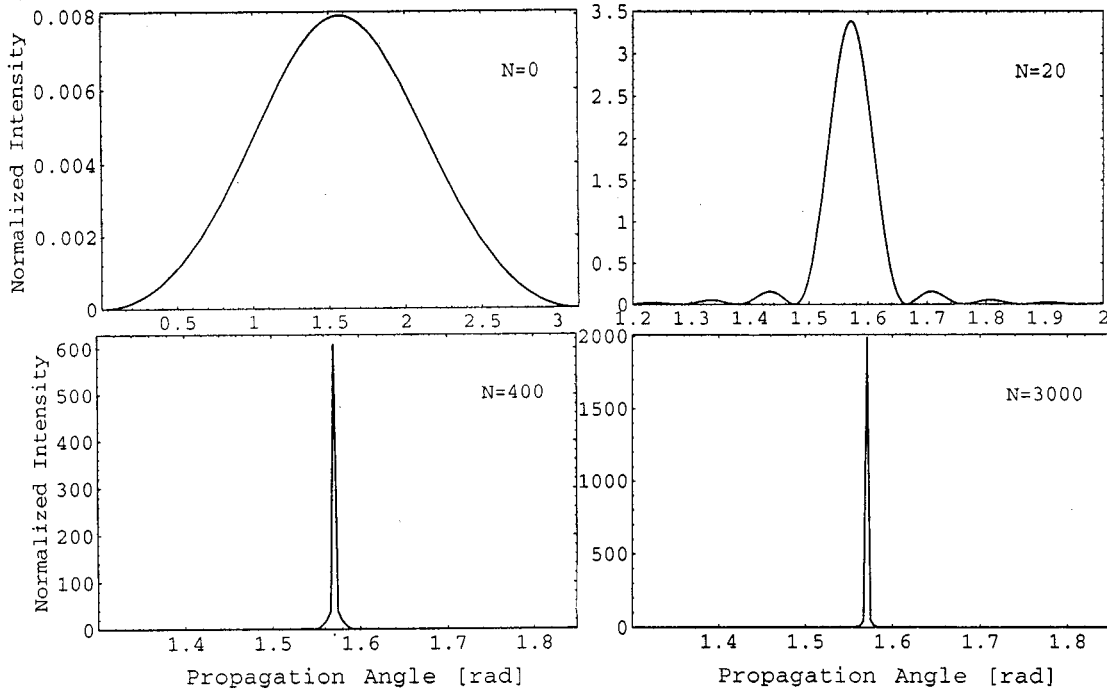


FIG. 5. External radiation patterns for a dipole perpendicular to the mirrors as in Fig. 3 but with mirror separation $d = \lambda/4$.

ence between the partially reflected emitted waves. The atomic dipole normal to the mirrors interacts with the mode whose polarization is orthogonal to the mirrors, and the emission is enhanced rather than inhibited. The enhancement factor of the peak radiated intensity in the steady state is obtained for $\theta = \pi/2$ as

$$\frac{I_{\perp}(\pi/2)}{I_0} = \frac{|T|^2(1+|R|)^2}{(1-|R|^2)^2} \cong \frac{4}{1-|R|^2} \quad (25)$$

for $|R|^2 \rightarrow 1$. The spontaneous emission enhancement factor is independent of the value of d for a dipole orthogonal to the mirrors, because of the term $\cos \theta = \cos(\pi/2) = 0$ that multiplies kd in Eqs. (6) and (7).

For $d = \lambda/4$, and in the limit $|R|^2 \rightarrow 1$, the normalized intensity distribution in the steady-state regime can be expressed as

$$\frac{I_{\perp}(\theta)}{I_0} = \frac{4}{\pi} \frac{|T|^2/\pi|R|}{(|T|^2/\pi|R|)^2 + \left(\theta - \frac{1}{2}\pi\right)^2} \cong 4\delta\left(\theta - \frac{\pi}{2}\right). \quad (26)$$

The total spontaneous emission rate of the atom, obtained from Eq. (11) with \parallel replaced by \perp and π replaced by $\pi/2$ in Eq. (17), is $\Gamma_{\perp} = 3\Gamma_0$. For $d \ll \lambda/2$, we set $kd \approx 0$ in Eqs. (6) and (7) and replace π by 0 in Eq. (17) to obtain the spontaneous emission rate for a general value of $|R|$, as

$$\Gamma_{\perp} = \Gamma_0 \frac{1+|R|}{1-|R|} \quad \text{for } d \ll \lambda/2. \quad (27)$$

The spontaneous emission rate of the dipole orthogonal to the mirrors tends to infinity when $|R|^2 \rightarrow 1$, in agreement with previous results [7,16]. It has been noted [16] that, since

the energy density of the quantum vacuum field is inversely proportional to the cavity volume, the atom-vacuum field coupling increases when $d \rightarrow 0$, leading to a divergence.

Apart from the perpendicular dipole with $d < \lambda/4$, the change in spontaneous emission rate from the free-space value caused by insertion of the atom in the planar cavity is limited to a factor of 3.

III. TRANSIENT AND STEADY-STATE FIELD DISTRIBUTIONS

In this section we obtain the dependence on mirror reflectivity of the characteristic time needed for the formation of the steady-state spatial intensity distribution emitted by an atomic dipole in a planar cavity. The most interesting case to analyze is a microcavity whose distance between the mirrors is $d = \lambda/2$ with the emitting dipole parallel to the x axis, where the time and N dependences of the emission are equivalent. It is shown in Sec. II A that the form of the emission lobe tends toward a tight concentration around the z axis for reflectivities tending to unity. From an analytical study of the dependences of the propagation angle of the emitted field on the time and the reflectivity in the weak-coupling regime, we can derive the mean time needed for the establishment of the transverse coherence length and mode volume in a planar cavity.

A. Angular divergence of the emitted radiation

We consider the radiation pattern in the xz plane, remembering that the spatial distribution becomes isotropic in the xy plane after a small number of initial reflections. We evaluate the lobe angular divergence as a function of N , and derive its dependence on the reflectivity of the mirrors. The normal-

ized radiated intensity distribution is given by Eq. (9) with $\phi=0$. The spontaneous emission is enhanced at $\theta=0$, with value

$$\frac{I_{\parallel}(0,N)}{I_0} = \frac{1+|R|}{1-|R|} (1-|R|^{2(N+1)})^2. \quad (28)$$

We limit our attention to very high reflectivities, $|R|^2 \rightarrow 1$ or $|T|^2 \rightarrow 0$, when the results of the Sec. II A show that $\theta \rightarrow 0$. The propagation angle θ at half the maximum height of the intensity distribution is derived from

$$\begin{aligned} & \frac{1+|R|^{4(N+1)}-2|R|^{2(N+1)}\cos(\pi(N+1)\theta^2)}{(1-|R|^2)^2+|R|^2\pi^2\theta^4} \\ &= \frac{(1-|R|^{2(N+1)})^2}{2(1-|R|^2)^2}, \end{aligned} \quad (29)$$

where the intensity expression on the left is obtained from Eq. (9) with $\phi=0$, and expanded in powers of θ . Only the leading terms in the limits of small θ and $|T|^2$ are retained and, in particular, the $\theta=0$ values of the final two factors in Eq. (9) are sufficient. It follows that

$$\begin{aligned} & \frac{1}{2}(1+|R|^{2(N+1)})^2-2|R|^{2(N+1)}\cos(\pi(N+1)\theta^2) \\ &= \frac{|R|^2\pi^2\theta^4}{2}\left(\frac{1-|R|^{2(N+1)}}{1-|R|^2}\right)^2. \end{aligned} \quad (30)$$

The angle in the remaining cosine is not small as N tends to large values, and this term cannot be expanded around $\theta=0$.

Consider first perfectly reflecting mirrors with $|R|^2 \rightarrow 1$, when Eq. (30) can be written

$$\cos x \cong 1 - (x^2/4) \quad \text{where} \quad x = \pi(N+1)\theta^2. \quad (31)$$

The solution $x=0$ is an artifact of the perfect-reflectivity limit, and we require a second solution close to $x=\pi$. Expansion of $\cos x$ around this value gives in first approximation:

$$\cos x \cong -1 + \frac{(\pi-x)^2}{2} = 1 - \frac{x^2}{4}. \quad (32)$$

This quadratic equation is readily solved, and the angular spread $\Delta\theta(N)$ of the emitted radiation is obtained from twice the field propagation angle θ at half maximum intensity as

$$\begin{aligned} \Delta\theta(N) &= 2\theta(N) \\ &= \frac{2}{\sqrt{\pi(N+1)}} \left(\frac{2\pi + (24 - 2\pi^2)^{1/2}}{3} \right)^{1/2} \approx \frac{1.88}{\sqrt{N+1}}. \end{aligned} \quad (33)$$

The limit of an ideal cavity is thus characterized by an angular divergence of the transmitted field that tends to zero as $N^{-1/2}$ as $N \rightarrow \infty$. Expression (33) is correct for relatively large values of N , compatible with the treatment of the co-

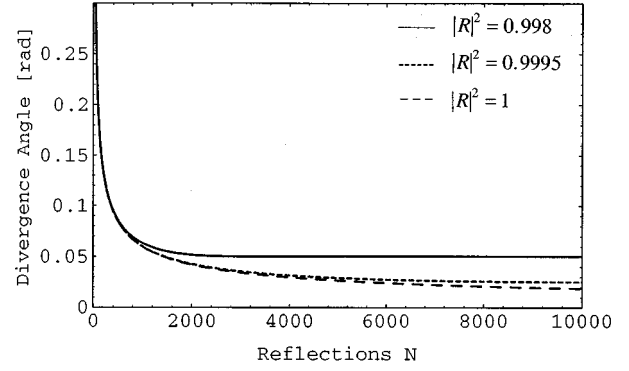


FIG. 6. Angular divergence of the radiation emitted by a dipole parallel to the mirrors after N reflections, for cavities with $d=\lambda/2$ and $|R|^2=0.998, 0.9995$, and 1.

sine term in Eq. (30). Nevertheless it turns out that Eq. (33) satisfies Eq. (32) within a good approximation even for moderate values such as $N \cong 50$.

The same form of expansion continues to provide a good approximation for the radiation pattern of a dipole placed in a lossy cavity with very high reflectivity mirrors. We shall find that the cavity field mode is established after a mean time corresponding to $N \gg 50$. Thus with $|R|^2$ close, but not necessarily equal to 1, expansion of Eq. (30) around $x=\pi$ gives a quadratic equation of the form, $ax^2+bx+c=0$, with

$$\begin{aligned} a &= \frac{|R|^2}{2(N+1)^2} \left(\frac{1-|R|^{2(N+1)}}{1-|R|^2} \right)^2 + |R|^{2(N+1)}, \\ b &= -2\pi|R|^{2(N+1)}, \\ c &= -\frac{1}{2} + (\pi^2-3)|R|^{2(N+1)} - \frac{1}{2}|R|^{4(N+1)}. \end{aligned} \quad (34)$$

The external angular divergence is now a function of $|R|$ obtained from

$$\Delta\theta(N,|R|) = \frac{2}{\sqrt{\pi(N+1)}} F(N,|R|), \quad (35)$$

with

$$F(N,|R|) = \left(\frac{-b + (b^2 - 4ac)^{1/2}}{2a} \right)^{1/2}. \quad (36)$$

The result given by Eq. (33) for the lossless cavity is recovered from Eq. (35) in the limit $|R|^2=1$. On the other hand, the steady-state limit obtained for $N \rightarrow \infty$ is

$$\Delta\theta(N,|R|) \rightarrow \frac{2}{\sqrt{\pi(N+1)}} \left[\frac{(N+1)^2(1-|R|^2)^{2/3}}{|R|^2} \right]^{1/4} \cong \frac{2|T|}{\sqrt{\pi}}, \quad (37)$$

in agreement with Eq. (13).

B. Analysis of the results

Figure 6 illustrates the variation of $\Delta\theta(N,|R|)$ with the number of reflections that the radiation undergoes in the cav-

ity before emission, obtained from Eq. (35), for three values of the mirror reflectivity, including perfect mirrors with $|R|^2=1$. Isolated values of $\Delta\theta(N,|R|)$ can also be obtained from the widths of the complete radiation patterns shown in Fig. 2, and these agree closely with the continuous curve for $|R|^2=0.998$. The steady-state limits have been achieved at the right-hand side of the figure for the two lossy cavities, but the divergence angle for the perfect cavity continues to fall in accordance with Eq. (33).

The damping rate of a lossy planar cavity for normal propagation with $\theta\cong 0$ is usually defined as

$$\Gamma_c = c|T|^2/d, \quad (38)$$

and the associated *cavity storage time* (or cavity photon lifetime) is given by

$$\tau_c = 1/\Gamma_c = d/c|T|^2 = \langle N \rangle d/c, \quad (39)$$

where the mean number of reflections of the field before emission is defined approximately as

$$\langle N \rangle \cong 1/|T|^2. \quad (40)$$

Note that $\langle N \rangle = 500$ for mirrors with reflectivity $|R|^2 = 0.998$ and $\langle N \rangle = 2000$ for reflectivity $|R|^2 = 0.9995$. We remark that, since N represents the number of reflections that the field undergoes *after* the first round trip, $\langle N \rangle$ in Eq. (39) and (40) should strictly be written as $\langle N+1 \rangle$, but 1 can be ignored relative to $\langle N \rangle$ for the parameters adopted here. In terms of the above definitions, Fig. 6 shows that the mean characteristic time for establishment of the cavity field distribution is of the order of the storage time τ_c , in agreement with a previous estimate [20].

Expressing the cavity storage time as a function of the round-trip time from Eq. (8), we have

$$\tau_c = \langle N \rangle \tau_{\text{rt}}. \quad (41)$$

It is clear that, in contrast to spherical or one-dimensional cavities [1,2], the field pattern is established only after a time much greater than that of the first round trip. The higher the reflectivity, the more reflections the radiated field must undergo to completely establish its spatial pattern. With the above notation, the steady-state limit given by Eq. (37) is rewritten as

$$\Delta\theta = 2/\sqrt{\pi\langle N \rangle}. \quad (42)$$

In planar cavities with perfectly reflecting mirrors, the characteristic time τ_c tends to infinity, and this is associated with the infinite narrowing of the angular emission lobe represented by Eq. (14). These considerations have important consequences for the realization of the regime of strong coupling in a very high- Q planar cavity, and this is analyzed in Sec. V.

With azimuthal isotropy in the spatial intensity distribution, the solid angle of the emission lobe in the steady state is defined in a first approximation as

$$\Delta\Omega = \pi \left(\frac{\Delta\theta}{2} \right)^2 = \frac{1}{\langle N \rangle} = |T|^2, \quad (43)$$

where Eqs. (40) and (42) are used. The width $\Delta\omega_c$ of the spectrum transmitted by a Fabry-Pérot interferometer with $d=\lambda/2$, satisfies [8]

$$\Delta\omega_c/\omega_c = 1/f, \quad (44)$$

where f is the finesse of the microcavity defined as

$$f = \frac{\pi|R|}{1-|R|^2} \cong \frac{\pi}{1-|R|^2} = \frac{\pi}{|T|^2} \quad (45)$$

for reflectivities tending to unity. The solid angle [Eq. (43)] is thus proportional to the transmitted spectral width [Eq. (44)]. This suggests that the progressive establishment of the spatial intensity distribution, as a function of the number of field reflections, is accompanied by a similar progressive establishment of the spectral ‘‘pattern’’ of the emitted radiation. We have derived the spatial pattern of the emitted field for a well-defined emission wavelength λ , but the above remark implies that the atom learns about the spectral properties of the planar cavity only after a delay time of the order of τ_c , exactly as for the spatial field configuration.

C. Planar microcavity transverse coherence length and mode volume

From conventional diffraction theory, the diameter of the aperture that gives the angular width $\Delta\theta$ of the emission lobe outside the cavity is obtained from Rayleigh’s criterion as [8]

$$l_c \approx \lambda/\Delta\theta. \quad (46)$$

We can thus associate l_c with the transverse extension of the cavity-field distribution, also defined as the coherence length of the microcavity. From Eqs. (35) and (46), l_c is a function of the mirror reflectivity and the number of field reflections given by

$$l_c(N,|R|) \approx \frac{\lambda}{\Delta\theta(N,|R|)} \approx \frac{\lambda}{2} \frac{\sqrt{\pi(N+1)}}{F(N,|R|)}. \quad (47)$$

In the steady-state regime, with $N \rightarrow \infty$, the coherence length l_c is obtained with the use of Eqs. (37) and (45) as

$$l_c \approx \lambda \sqrt{\pi/2} |T| \sim \frac{1}{2} \lambda \sqrt{f}, \quad (48)$$

whose dependence on λ and f agrees with previous results [3,4,10,11,21]. The steady-state field distribution, with an effective radius $r_c = l_c/2$, is equivalent, in some respects, to a mode of the lossy planar cavity [21]. Its localized cylindrical field distribution contrasts with the usual plane-wave modes of infinite extent along the mirror surfaces described in Sec. II. The finiteness of the transverse dimension of the effective mode, equal to the coherence length, is a direct consequence of the finite loss of the cavity, which also yields the finite external divergence angle. It has been observed [22] that r_c is also the minimum radius of the mirrors needed to support the mode.

Note that for a dipole in a lossless cavity, Eqs. (33) and (47) give

$$l_c \sim \lambda \sqrt{\pi(N+1)} \quad (49)$$

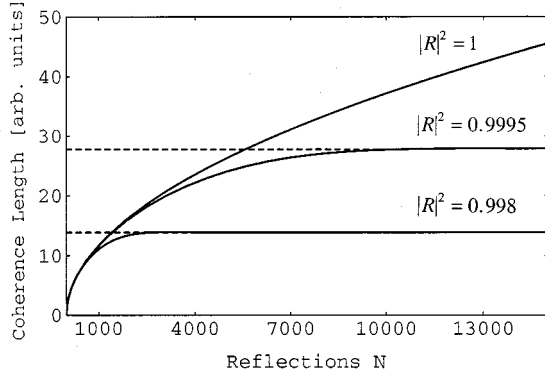


FIG. 7. Evolution of the transverse coherence length as a function of N , or equivalently of the time, for the mirror reflectivities shown. The broken lines show the steady-state values for the lossy cavities.

and $l_c \rightarrow \infty$ when $N \rightarrow \infty$. In a resonant planar cavity with perfect mirrors, the mode of the electromagnetic field is thus infinitely extended in the plane of the mirrors, corresponding to the zero divergence angle of the emission lobe. As we have seen, the mean time τ_c necessary for the establishment of the mode also tends to infinity. The evolution of l_c as a function of N is shown in Fig. 7 for three values of the mirror reflectivity.

The approximate volume of the steady-state radiative mode in a planar microcavity is

$$V \approx \pi \left(\frac{l_c}{2} \right)^2 d \approx \frac{\pi^2 \lambda^3}{32 |T|^2} \sim \frac{\lambda^3}{|T|^2} \quad \text{for } d = \frac{1}{2} \lambda. \quad (50)$$

For high-reflectivity mirrors, this is very much larger than the mode volume in confocal cavities, where $V_{\text{conf}} \sim \lambda^3$ [23].

IV. SPONTANEOUS EMISSION BY AN ATOM NEAR A PLANE MIRROR

It is instructive to compare the dynamics of the establishment of the electromagnetic field radiated by a dipole in a planar cavity with that radiated by a dipole placed in front of a single plane mirror. The system is equivalent to a cavity constituted by two mirrors, one of which is perfectly transmitting. The formalism is based on that of Sec. II, where the right-hand mirror shown in Fig. 1 is removed by setting $R_2 = 0$, and $T_2 = 1$. The following derivation of the transient regime of the spatial evolution confirms previous results [6], and it gives an interesting comparison with the planar cavity. For simplicity we assume that the atomic dipole is parallel to the plane of the mirror, for example parallel to the x axis.

In the system with a single mirror, the Airy function (5) and its expansion (7), which describes the N -dependent evolution of the radiation pattern, both equal unity. The contributions to the spatial intensity distribution, and similarly to the spontaneous emission rate, come essentially from the interference between the field radiated to the right and the counterpropagating field reflected by the mirror on the left. Of course the Airy function reduces to unity because no multiple reflections can physically occur in a system with a single mirror.

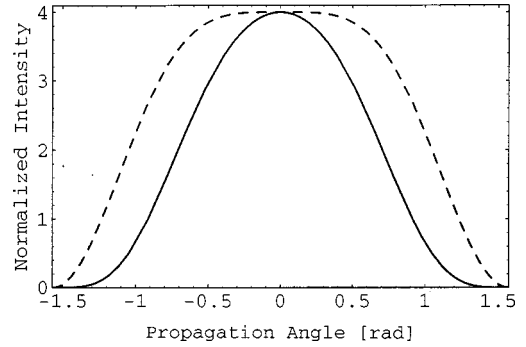


FIG. 8. Radiation pattern for a dipole parallel to a single perfect mirror at a distance $d/2 = \lambda/4$. The continuous and broken curves refer to the zx and yz planes, respectively.

When the remaining left-hand mirror is perfectly reflecting, the normalized radiated intensity in the steady-state regime is derived from the formalism of Sec. II, or from classical wave-interference considerations, as

$$I_{\parallel}(\theta, \phi)/I_0 = 2\{1 - \cos(kd \cos \theta)\} \{\sin^2 \phi + \cos^2 \theta \cos^2 \phi\}. \quad (51)$$

Both the s - and p -polarized field components contribute to the spontaneous emission, as for a dipole placed in a cavity and oriented parallel to the mirrors. We assume that the atom is placed at a distance from the mirror given by $d/2 = \lambda/4$, where the spontaneous emission rate is enhanced. The radiation pattern in the horizontal zx plane is given by

$$I_{\parallel}(\theta, 0)/I_0 = 2\{1 - \cos(\pi \cos \theta)\} \cos^2 \theta, \quad (52)$$

while the radiation pattern in the vertical yz plane is

$$I_{\parallel}(\theta, \pi/2)/I_0 = 2\{1 - \cos(\pi \cos \theta)\}. \quad (53)$$

The spatial intensity distribution is thus inhomogeneous, because of the different contributions from the two polarizations. The radiation patterns as functions of the propagation angle are shown in Fig. 8.

The transient regime in the single-mirror system occurs during the round-trip time or more exactly during the generalized round-trip time τ_{ref} defined in Eq. (8). The steady-state interference pattern is now established after the waves propagating toward the mirror have been reflected back to the atom. Thus the dipole, emitting initially as in free space, needs only the information from the reflected wave in order to adapt its further evolution. Because of the enhancement at $d/2 = \lambda/4$, the angular divergence of the emission is slightly narrowed with respect to free space, although the effect is much smaller than that observed for a dipole in a cavity, where multiple reflections generate the progressive angular narrowing of the radiation. The pattern in Fig. 8 is very similar to that of a dipole placed in a symmetrical cavity (and parallel to the x axis) after the first reflection of the field on the mirrors.

The spontaneous emission rate is given by Eq. (11) with substitution of the normalized intensity from Eq. (51), except that an additional factor of $\frac{1}{2}$ must be inserted to allow for the restriction of the radiation to half of space. For a general position of the dipole,

$$\Gamma_{\parallel} = \Gamma_0 \left(1 - \frac{3 \sin kd}{2 kd} + \frac{3 \sin kd}{2 (kd)^3} - \frac{3 \cos kd}{2 (kd)^2} \right), \quad (54)$$

in agreement with previous results [5,7,15]. When $d/2 = \lambda/4$, we obtain

$$\Gamma_{\parallel} = \Gamma_0 \left(1 + \frac{3}{2\pi^2} \right), \quad (55)$$

showing a slight enhancement over the free-space spontaneous emission rate.

V. STRONG-COUPPLING REGIME IN SYMMETRICAL MICROCAVITIES

The results obtained in preceding sections are important for evaluating the possibilities of accessing the strong-coupling regime and of observing Rabi oscillations in planar high- Q resonant cavities. Here we point out relevant consequences of our results for planar microcavities and we highlight the important differences from the confocal cavities used in most QED experiments.

A. Confocal cavity: ideal system for QED experiments

For a dipole excited at time $t=0$, we have seen that the atom radiates as in free space for $0 < t < \tau_{\text{rt}}$. If the round-trip time is the characteristic delay time necessary for the adaptation of the electromagnetic field to the environment, as in confocal, spherical, or one-dimensional cavities, then an abrupt change in the atomic dynamics occurs for $t \geq \tau_{\text{rt}}$ [1,2]. For an emitting atom in these cavities, after the first round trip of the light, interference effects occur that result ‘‘either in an enhancement or reduction of the emission rate or in a periodic exchange of excitation between the atom and the cavity field’’ [2]. Then, depending on the value of the Rabi period with respect to the microcavity storage time τ_c defined in Eq. (39) and the spontaneous emission lifetime τ_{rad} , either the weak or strong-coupling regime can be realized.

The Rabi frequency characterizes the coupling between the two-level atom and the resonant cavity field mode in the strong-coupling regime. It is defined, in general, as

$$\Omega = \frac{2\mu}{\hbar} \left(\frac{\hbar \omega_0}{2\epsilon_0 V} \right)^{1/2}, \quad (56)$$

where μ is the electric-dipole matrix element of the atomic transition of frequency ω_0 , and V is the effective volume of the microcavity; or, equivalently, the mode volume assumed in steady-state conditions. The Rabi frequency is related to the free-space spontaneous emission rate Γ_0 by

$$\Omega^2 = \frac{4\omega_0\mu^2}{2\epsilon_0\hbar V} = \frac{6\pi c^3}{\omega_0^2} \frac{1}{V} \Gamma_0, \quad (57)$$

and Ω can be evaluated when the radiative decay rate is known and the field mode volume V can be reasonably estimated. For a half-wavelength resonant cavity with $\tau_{\text{rad}} \gg \tau_{\text{rt}}$, the emission for times $t \geq \tau_{\text{rt}}$ occurs in a single longitudinal mode of volume V , and the vacuum Rabi frequency Ω is well defined at the moment of the photon emission. The spatial and spectral confinement of the emitted radiation is a

characteristic feature of the structure of the confocal microcavity mode spectrum [24,25].

The cavities used in experiments with Rydberg atoms have very high-quality factors [26–29] in order to observe the effects of coherent coupling. The atomic transition of a two-level Rydberg atom prepared with a very large quantum number lies in the millimeter wave region, with parameter values

$$\omega_0 \cong 10^{10} - 10^{11} \text{ s}^{-1} \quad \text{and} \quad \Gamma_0 = 10^5 - 10^6 \text{ s}^{-1}. \quad (58)$$

For the cavity parameters, we take a mode volume of the order of $5\lambda^3$, as reported in Ref. [23], and typical values of Ω and Γ_c are

$$\Omega = 10^6 - 10^7 \text{ s}^{-1} \quad \text{and} \quad \Gamma_c \approx 10^3 - 10^4 \text{ s}^{-1}, \quad (59)$$

where the Rabi frequency is obtained from Eq. (57). The cavity Q can thus be of order 10^8 and the inequalities $\Omega \gg \Gamma_c, \Gamma'_0$ are satisfied, where Γ'_0 is a residual radiative decay rate that excludes emission into the selected mode. Equivalently, τ_c is much longer than the period $1/\Omega$ of Rabi oscillation. The strong-coupling regime can be achieved, and this is confirmed by experiment [27,28]. Confocal microcavities provide ideal systems for the realization of QED experiments in the strong-coupling limit, as initially introduced in the Jaynes-Cummings model (JCM) [30].

When $\tau_{\text{rad}} \gg \tau_{\text{rt}}$, the emitted field for $t \leq \tau_{\text{rt}}$ is built up during the very initial dynamics of the radiative process. The mean energy E in the cavity electromagnetic field at $t = \tau_{\text{rt}}$ is, therefore,

$$E(\tau_{\text{rt}}) = \hbar \omega_0 (1 - \exp(-\tau_{\text{rt}}/\tau_{\text{rad}})) \approx \hbar \omega_0 (\tau_{\text{rt}}/\tau_{\text{rad}}) \ll \hbar \omega_0. \quad (60)$$

The atom is still nearly totally excited at time $t = \tau_{\text{rt}}$, but because of this infinitesimally small quantity of energy released during the first round-trip time, the dipole is able to feel the boundaries and adapt its further evolution to the cavity environment. For perfect mirrors and a configuration for which the spontaneous decay is inhibited, expression (60) represents the cavity-field energy in the steady state. Fearn *et al.* [6] showed that this steady-state field energy has important consequences for the immediate detection of photons upon removal of one of the cavity mirrors. Kauranen *et al.* [31] confirmed the presence of the steady-state field in a system equivalent to a dipole sheet placed in front of a single mirror.

B. Planar microcavity

In contrast to the confocal cavity, the transient regime of the atomic dynamics in a planar microcavity in the weak-coupling regime occurs over a mean period of duration τ_c . The dipole acquires complete information about the boundaries progressively, by means of many successive reflections of the radiation. The realization of JCM experiments requires that the atomic emission should occur after the effective mode in the cavity is established, that is $\tau_{\text{rad}} \gg \tau_c$, or equivalently $\Gamma_0 \ll \Gamma_c$ in terms of the radiative and cavity decay rates. Only the weak-coupling regime can be accessed when these inequalities are satisfied, without any possibility of periodical exchange of energy between the atom and the radia-

tion field. The dipole again radiates as in free space for $0 < t < \tau_{\text{rt}}$, but the spontaneous emission rate now undergoes a slow progressive modification after each round trip of the emitted radiation for times $\tau_{\text{rt}} \leq t \leq \tau_c$.

For a half-wavelength planar cavity, with transition frequency $\omega_0 = \pi c/d$, substitution of the cavity decay rate from Eq. (38) and the mode volume from Eq. (50) into Eq. (57) gives

$$\Omega^2 = \frac{24}{\pi^3} \Gamma_c \Gamma_0 \approx \Gamma_c \Gamma_0. \quad (61)$$

This simple relation shows that the value of the vacuum Rabi frequency of the planar microcavity lies close to the geometric mean of the cavity decay rate and the free-space atomic spontaneous emission rate. Thus the conditions of strong atom-field coupling and a high- Q cavity needed for the observation of vacuum Rabi oscillations imply the inequality:

$$\Gamma_0 \gg \Omega \gg \Gamma_c. \quad (62)$$

There is, however, a contradiction in these relations, as the Rabi frequency Ω itself assumes the value used in the derivation of Eq. (61) only after the delay time τ_c necessary for the field in the cavity to reach its steady state. Inequality (62), equivalent to $\tau_{\text{rad}} \ll \tau_c$, implies that the radiation pattern is still in its transient regime at the moment of emission, and Ω cannot be written as in Eq. (56) since the mode volume V is not yet established. The atom in a planar cavity cannot acquire complete information about its environment until well after the cavity decay time τ_c has elapsed, when the probability that the photon has been transmitted through the mirrors is very high. The probability of reabsorption of the photon by the atom is accordingly very low, and the regime of strong atom-field coupling with Rabi oscillations cannot be accessed. Although Gießen *et al.* [2] analyzed the ‘‘multimode’’ JCM with the possibility of Rabi oscillations, their cavity was one dimensional with a mode ‘‘volume’’ established after the round-trip time τ_{rt} .

For dielectric mirrors with very high reflectivity $|R|^2 > 0.9999$ [9] and an optical transition in the visible region, typical parameter values are

$$\Gamma_0 \approx 10^8 \text{ s}^{-1}, \quad \Omega \approx 3 \times 10^9 \text{ s}^{-1} \quad \text{and} \quad \Gamma_c \approx 10^{11} \text{ s}^{-1}, \quad (63)$$

and these satisfy

$$\Gamma_0 \ll \Omega \ll \Gamma_c, \quad (64)$$

which is the reverse of the triple inequality in Eq. (62). The same inequality (64) is satisfied, but more weakly, for mirrors of the same reflectivity but atomic parameters corresponding to transitions of Rydberg atoms in the millimeter wave range. The difficulties in achieving the strong-coupling regime are caused essentially by the intrinsic multimode spectrum of the planar cavity, where there is a dense continuum of nondegenerate transverse modes associated with each discrete longitudinal mode [24,25,32]. The existence of a transverse confinement of the field excitation within an effective mode radius r_c , discussed in Sec. III C, does not

significantly affect previous conclusions that strong coupling and Rabi oscillations cannot be achieved in planar cavities [16,25].

For the weak-coupling regime with $\tau_{\text{rad}} \gg \tau_c$, that is more readily accessible, it remains true that the radiation pattern is established during the very initial dynamics of the radiative process, with the field energy at time $t = \tau_c$ given by

$$E(\tau_c) = \hbar \omega_0 (1 - \exp(-\tau_c / \tau_{\text{rad}})) \approx \hbar \omega_0 (\tau_c / \tau_{\text{rad}}) \ll \hbar \omega_0. \quad (65)$$

Note that Eq. (65) is a more approximate expression than Eq. (60), since the atomic decay time itself undergoes variations for $\tau_{\text{rt}} \leq t \leq \tau_c$. Nevertheless, it follows from the decay rates for a half-wavelength resonant cavity obtained in Secs. II A and II B, that the energy inequality in Eq. (65) is valid.

C. Other varieties of cavity

The planar and confocal cavities are two special cases of a series of stable symmetric cavities characterized by the relative values of the cavity length d and the radius of curvature R of the spherical mirrors, in the range [24]

$$d/2 \leq R \leq \infty. \quad (66)$$

The infinite radius of curvature corresponds to the planar cavity, a radius equal to the cavity length to the confocal cavity, and a radius equal to half the cavity length to the spherical or concentric cavity. The planar and confocal cavities have been discussed in detail, and here we make some comments on other kinds of cavity that are sometimes used in calculations or experiments.

The planar cavity is the limit of a symmetrical cavity as the mirror radii of curvature tend to infinity. For a radius of curvature R that is much greater than the cavity length d , but is not infinite, the mode continua of the strictly planar cavity break up into discrete modes with the characteristic transverse separation [24]

$$\Delta \omega = (2c^2/Rd)^{1/2}. \quad (67)$$

Our conclusions for the planar cavity continue to apply when $\Delta \omega$ is small compared with the atomic and cavity linewidths, so that the continua of transverse modes survive. In the opposite limit of a $\Delta \omega$ that is much larger than the linewidths but much smaller than the longitudinal mode separations, as in recent experiments on single-atom-cavity QED [33,34], the planar theory no longer applies; the conditions in such cases resemble those of the confocal cavity and strong-coupling conditions may be achieved. For intermediate values of $\Delta \omega$, it is necessary to perform a detailed analysis of the emission in order to evaluate the transient behavior and the possibilities of observing Rabi oscillations.

The concentric microcavity with $d = 2R$ also has continuous distributions of modes when the transverse field variations are included. The transverse-mode continua now extend from the low-frequency sides of the discrete longitudinal frequencies, and transient effects similar to those found here for the strictly planar cavity could in principle occur. There is however, an important distinction between the planar and concentric microcavities in terms of their mode cross sections [24]. For the planar cavity, the

steady-state mode has the large circular transverse cross section discussed in Sec. III C, both in the planes of the mirrors and in the plane of the atom at the center of the cavity, leading to weak coupling between the atomic dipole and the field mode. For the concentric cavity, the modes also have a large cross section, or spot size, at the mirrors but a very small cross section at the position of the atom, leading to stronger atom-field coupling. With the effects of the transverse modes suppressed and only radially varying mode functions, the concentric cavity has a mode spectrum and transient effects similar to those of a one-dimensional cavity [1]. The nearly concentric cavity also has a discrete transverse-mode spectrum, analogous to that of the nearly planar cavity discussed above, and this provides another means of achieving single-mode coupling.

Discrete-mode conditions can thus be realized in a wide variety of cavity configurations with strong coupling to the radiating atom available in systems that have small mode cross sections, and thus strong intensities, at the atomic position. Nevertheless, confocal cavities are adopted in the majority of experiments because of their natural single-mode confinement, which occurs both spatially and spectrally.

VI. CONCLUSIONS

The effects of environment on the spontaneous emission characteristics of an excited atom form an important part of the study of the quantum-electrodynamical vacuum [35]. One aspect of the emission is its modification from free-space form as the atom becomes “aware” of its surroundings by the reflection of initially emitted radiation back to the atom. The atomic decay thus displays an initial transient behavior up to some time that characterizes the complete awareness of its environment by the atom. Previous calculations [1,2,6] have treated atoms in essentially one-dimensional cavities of length d , where the transient regime extends up to times of the order of the round-trip time $\tau_{\text{rt}} = d/c$. Such theories apply to real cavities whose geometries produce modes with well-defined spatial configurations and isolated frequencies as, for example, in the confocal cavity.

Planar cavities, on the other hand, have continuous distributions of transverse modes associated with each longitudinal frequency and they cannot be treated realistically by any one-dimensional theory. We accordingly use a three-dimensional theory to study the emission of radiation by an atom excited at time $t=0$. The system parameters are assumed to satisfy conditions of weak atom-field coupling. For a half-wavelength high- Q cavity with $d=\lambda/2$, the spatial distribution of the emission retains its free-space form for times up to the round-trip time τ_{rt} but it progressively changes to a narrow lobe, for a transition dipole moment parallel to the mirrors, or to a thin sheet, for a dipole moment perpendicular to the mirrors. The distribution of the emission by an excited atom in a quarter-wavelength cavity with $d=\lambda/4$ again tends to a thin sheet for a perpendicular dipole, but the emission is now inhibited for the parallel dipole.

The transient regime is particularly well characterized for a parallel dipole in a $d=\lambda/2$ cavity where, in contrast to the effectively one-dimensional cavity, it extends up to times of the order of the cavity decay time $\tau_c = d/c|T|^2$, where T is the mirror transmission coefficient. The changing spatial dis-

tributions of the emitted radiation are observable in principle, but the experiment is difficult in practice because only a small fraction of the initial excitation energy of the atom is radiated over the brief time scale τ_c . The spatial distribution of the internal field of the cavity at the end of the transient regime has a transverse extent of the order of the coherence length $l_c \approx \lambda/|T|$, which is related to the angular spread of the external radiation by Rayleigh’s criterion. The coherence length was originally defined as the minimum separation distance of pairs of atoms for which correlation effects occur [3], and it has also previously been identified as the effective transverse dimension of the spontaneous-emission field volume in the steady state [4]. The planar microcavity provides a versatile system for the controlled variation and measurement of such correlations [36,37].

Planar cavities do not, however, provide suitable systems for the study of the Rabi oscillations that occur in the strong-coupling regimes of effectively one-dimensional cavities. Thus, the identification of a finite transverse dimension for the internal field excitation does not alter previous conclusions that strong coupling cannot be achieved and Rabi oscillations cannot be observed [16,25]. The difficulty essentially arises because the time τ_c taken to establish the steady field distribution within the cavity is the same as the characteristic time for the loss of the initial atomic excitation energy to the external field, when inequality (62) is satisfied. The single quantum of energy in the complete system is thus unavailable for re-excitation of the atom, as needed for the occurrence of Rabi oscillations.

Our account of transient spontaneous emission is based on calculations of the time-dependent radiation of electromagnetic waves by an atom excited at time $t=0$. The effects of a cavity environment become apparent over the times needed for the radiated waves to experience the detailed structures of the cavity mirrors. An alternative approach often used to obtain environmental modifications of the atomic emission is to calculate the density of electromagnetic field modes at the position of the atom and at the frequency ω of its transition. The emission rate is taken to be proportional to this mode density and the radiation pattern is determined by superposition of the amplitudes of the modes excited in the emission process. It is not immediately clear how the initial transient behavior of the emission appears in this alternative approach.

Consider first the confocal microcavity, whose mode density is comblike with teeth of uniform spacing $\pi c/d$ and width Γ_c , assumed much smaller than the mode spacing. The initial transient behavior occurs in the mode-density approach because of the spread of emission frequencies around ω at early times. Thus, according to the energy-time uncertainty relation (see, for example, Refs. [38,39]), the emission has a frequency spread of order $1/\Delta t$ at time Δt . It follows that for

$$\frac{1}{\Delta t} \gg \frac{\pi c}{d} \quad \text{or} \quad \Delta t \ll \frac{\tau_{\text{rt}}}{\pi}, \quad (68)$$

the emission occurs into very many modes to give a free-space rate and pattern. However, when Δt is comparable to or greater than τ_{rt} the emission is confined to a frequency range much smaller than the mode spacing and the full ef-

fects of the cavity confinement are apparent. The transient regime thus extends over times of order τ_{π} as in the previous calculations.

For the planar microcavity, we consider only transition dipole moments parallel to the mirrors, where the appropriate mode density approximately vanishes for frequencies up to the order of the cavity linewidth Γ_c below $\pi c/d$. The mode density then displays a series of continua that extend to higher frequencies, with sharp edges at odd integer multiples of $\pi c/d$; these edges have decaying tails with lengths of order Γ_c on their low-frequency sides. The explanation of the transient behavior in the mode-density approach is similar to that for the confocal microcavity for times much shorter than τ_{π} , when emission occurs into many of the continua to give again a free-space-like rate and pattern. For longer times we consider the example illustrated in Fig. 2, where $d = \lambda/2$ and the transition frequency ω lies just within the edge of the first mode-density continuum. For times much longer than τ_{π} , but much smaller than τ_c , the emitted frequencies lie partly in the region of nearly zero mode density below the edge and partly within the first continuum above the edge. The density of accessible modes continues to change with increasing time until their spread reduces to the

width of the continuum edge, equal to Γ_c , when a steady state is achieved. The mode-density approach thus predicts a transient regime that extends up to times of the order of the cavity storage time τ_c , which again agrees with the previous calculations.

In summary, the planar and one-dimensional cavities differ markedly in the time scales of their transient regimes in spontaneous emission by an excited atom. Beyond its transient regime, the planar cavity allows studies of transverse coherence effects, which do not occur in the effectively one-dimensional cavities. On the other hand, the latter allow observation of the Rabi oscillations for achievable values of the system parameters, while these oscillations cannot be realized in the planar cavity.

ACKNOWLEDGMENTS

The research was performed under subcontract with the University of Rome ‘‘La Sapienza,’’ supported by the European Community Network on Microlasers and Cavity QED (ERBFMRXCT96-0066). We acknowledge very useful discussions with Francesco De Martini, Paolo Mataloni, Ralph Steidl, and Andreas Sizmann.

-
- [1] J. Parker and C. R. Stroud, *Phys. Rev. A* **35**, 4226 (1987).
 - [2] H. Gießen, J. D. Berger, G. Mohs, P. Meystre, and S. F. Yelin, *Phys. Rev. A* **53**, 2816 (1996).
 - [3] F. De Martini, M. Marrocco, and D. Murra, *Phys. Rev. Lett.* **65**, 1853 (1990).
 - [4] K. Ujihara, *Jpn. J. Appl. Phys., Part 2* **30**, L901 (1991).
 - [5] F. De Martini, *Phys. Lett. A* **115**, 421 (1986).
 - [6] H. Fearn, R. J. Cook, and P. W. Milonni, *Phys. Rev. Lett.* **74**, 1327 (1995).
 - [7] F. De Martini, M. Marrocco, P. Mataloni, L. Crescentini, and R. Loudon, *Phys. Rev. A* **43**, 2480 (1991).
 - [8] M. Born and E. Wolf, *Principles of Optics*, 6th ed. (Cambridge University Press, Cambridge, 1997).
 - [9] S. Ciancaleoni, P. Mataloni, O. Jedrkiewicz, and F. De Martini, *J. Opt. Soc. Am. B* **14**, 1556 (1997).
 - [10] Y. Yamamoto, S. Machida, and G. Björk, *Opt. Quantum Electron.* **24**, S215 (1992).
 - [11] K. Ujihara, A. Nakamura, O. Manba, and X.-P. Feng, *Jpn. J. Appl. Phys., Part 1* **30**, 3388 (1991).
 - [12] G. Barton, *Proc. R. Soc. London, Ser. A* **320**, 251 (1970).
 - [13] M. R. Philpott, *Chem. Phys. Lett.* **19**, 435 (1973).
 - [14] S. D. Brorson, H. Yokoyama, and E. P. Ippen, *IEEE J. Quantum Electron.* **26**, 1492 (1990).
 - [15] E. A. Hinds, *Adv. At., Mol., Opt. Phys.* **28**, 237 (1991); **2**, 1 (1994).
 - [16] S. M. Dutra and P. L. Knight, *Phys. Rev. A* **53**, 3587 (1996); *Opt. Commun.* **117**, 256 (1995).
 - [17] G. Björk, *IEEE J. Quantum Electron.* **30**, 2314 (1994).
 - [18] P. W. Milonni and P. L. Knight, *Opt. Commun.* **9**, 119 (1973).
 - [19] J. P. Dowling, M. O. Scully, and F. De Martini, *Opt. Commun.* **82**, 415 (1991).
 - [20] P. Stehle, *Phys. Rev. A* **2**, 102 (1970).
 - [21] T. Enomoto, T. Sasaki, K. Sekiguchi, Y. Okada, and K. Ujihara, *J. Appl. Phys.* **80**, 6595 (1996).
 - [22] N. Koide and K. Ujihara, *Opt. Commun.* **111**, 381 (1994).
 - [23] S. Haroche and J. M. Raimond, *Adv. At., Mol., Opt. Phys.* **20**, 347 (1985).
 - [24] A. E. Siegman, *Lasers* (University Science Books, Mill Valley, CA, 1986).
 - [25] I. Abram and J. L. Oudar, *Phys. Rev. A* **51**, 4116 (1995).
 - [26] Y. Kaluzny, P. Goy, M. Gross, J. M. Raimond, and S. Haroche, *Phys. Rev. Lett.* **51**, 1175 (1983).
 - [27] G. Rempe, H. Walther, and N. Klein, *Phys. Rev. Lett.* **58**, 353 (1987).
 - [28] M. Brune, F. Schmidt-Kaler, A. Maali, J. Dreyer, E. Hagley, J. M. Raimond, and S. Haroche, *Phys. Rev. Lett.* **76**, 1800 (1996).
 - [29] M. Weidinger, B. T. H. Varcoe, R. Heerlein, and H. Walther, *Phys. Rev. Lett.* **82**, 3795 (1999).
 - [30] E. T. Jaynes and F. W. Cummings, *Proc. IEEE* **51**, 89 (1963).
 - [31] M. Kauranen, Y. Van Rompaey, J. J. Maki, and A. Persoons, *Phys. Rev. Lett.* **80**, 952 (1998).
 - [32] S. D. Brorson, in *Spontaneous Emission and Laser Oscillation in Microcavities*, edited by H. Yokoyama and K. Ujihara (CRC Press, Boca Raton, FL, 1995), p. 151.
 - [33] C. J. Hood, M. S. Chapman, T. W. Lynn, and H. J. Kimble, *Phys. Rev. Lett.* **80**, 4157 (1998).
 - [34] P. Münstermann, T. Fischer, P. W. H. Pinkse, and G. Rempe, *Opt. Commun.* **159**, 63 (1999).
 - [35] P. W. Milonni, *The Quantum Vacuum* (Academic, Boston, 1994).
 - [36] A. Aiello, F. De Martini, M. Giangrosso, and P. Mataloni, *Quantum Semiclass. Opt.* **7**, 677 (1995).
 - [37] E. De Angelis, F. De Martini, and P. Mataloni (unpublished).
 - [38] A. Messiah, *Quantum Mechanics* (North-Holland, Amsterdam, 1970), Vol. 2, p. 733.
 - [39] J. J. Sakurai, *Modern Quantum Mechanics* (Benjamin/Cummings, Menlo Park, CA, 1985), p. 329.